Cellular Physiology and Biochemistry

Cell Physiol Biochem 2018;49:1577-1588
DOI: 10.1159/000493460
Published online: 13 September, 2018
Accepted: 4 September, 2018

Original Paper

The *in Vitro* Effect of Polyvinylpyrrolidone and Citrate Coated Silver Nanoparticles on Erythrocytic Oxidative Damage and Eryptosis

Zannatul Ferdous[a] Sumaya Beegam[a] Saeed Tariq[b] Badreldin H Ali[c] Abderrahim Nemmar[a]

[a]Department of Physiology, College of Medicine and Health Sciences, United Arab Emirates University, Al Ain, [b]Department of Anatomy, College of Medicine and Health Sciences, United Arab Emirates University, Al Ain, UAE, [c]Department of Pharmacology and Clinical Pharmacy, College of Medicine and Health Sciences, Sultan Qaboos University, Al-Khod, Oman

Key Words
Silver nanoparticles • Coating • Erythrocytes • Oxidative stress • Eryptosis

Abstract
Background/Aims: Silver nanoparticles (AgNPs) are increasingly used as antimicrobial agents and drug carriers in various biomedical fields. AgNPs can encounter erythrocytes either directly following intravenous injection, or indirectly via translocation from the site of administration. However, information regarding the pathophysiological effects and possible mechanism of action of AgNPs on the erythrocytes are still inadequately studied. Thus, the aim of our study was to investigate the mechanism underlying the effect of coating and concentration of AgNPs on mouse erythrocytes *in vitro*. ***Methods:*** We studied the interaction of polyvinylpyrrolidone (PVP) and citrate (CT) coated AgNPs (10 nm) at various concentrations (2.5, 10, 40 µg/ml) with mouse erythrocytes *in vitro* using various techniques including transmission electron microscopy (TEM), hemolysis, and colorimetric measurement of markers of oxidative stress comprising malondialdehyde (MDA), reduced glutathione (GSH), and catalase (CAT). Intracellular calcium (Ca^{2+}) was determined using Fura 2AM fluorescence. Annexin V was quantified using ELISA and the caspase 3 was determined both flurometrically and by western blot technique. ***Results:*** Following incubation of the erythrocytes with AgNPs, both PVP- and CT- AgNPs induced significant and dose - dependent increase in hemolysis. TEM revealed that both PVP- and CT- AgNPs were taken up by erythrocytes. The erythrocyte susceptibility to lipid peroxidation measured by MDA was significantly increased in both PVP- and CT- AgNPs. The concentration of GSH and CAT activity were significantly decreased by both types of AgNPs. Additionally, PVP- and CT- AgNPs significantly increased intracellular Ca^{2+} in a dose -dependent manner. Likewise, the concentration of the cellular protein annexin

Abderrahim Nemmar
Department of Physiology, United Arab Emirates University
P.O. Box 17666, Al Ain (United Arab Emirates)
Tel. +971-37137533, Fax +971-37671966, E-Mail anemmar@uaeu.ac.ae

V was significantly and dose - dependently enhanced by both types of AgNPs. Furthermore, PVP- and CT- AgNPs induced significant increase in calpain activity in incubated erythrocytes. ***Conclusion:*** We conclude that both PVP- and CT- AgNPs causes hemolysis, and are taken up by erythrocytes. Moreover, we demonstrated that AgNPs induces oxidative stress and eryptosis. These findings provide evidence for the potential pathophysiological effect of PVP- and CT- AgNPs on erythrocyte physiology.

Introduction

Nanotechnology refers to the science which deals with particles that are less than 100 nm in size at least in one dimension [1-3]. In recent years, nanotechnology has gained huge popularity due to its unique physiochemical properties such as small size, large surface area to volume ratio, high reactivity, high carrier capacity and easy variation of surface properties [2]. Engineered nanoparticles (NPs) are being increasingly used for various biomedical purposes such as drug delivery, antimicrobial agents, molecular imaging and biomedical sensing [4, 5].

Silver nanoparticles (AgNPs) are among the most popular NPs known for their strong antimicrobial and disinfectant properties [6, 7]. The antibacterial activity of AgNPs has led to their extensive use in various household products such as self-sanitizing toothbrushes and bacteria - resistant stuffed toys. Some of the other applications of AgNPs include their use as catalysts, optical sensors of zeptomole (10^{-21} concentration), and in electronics and textile engineering, as bactericidal agents and as therapeutic agents in medical products such as wound dressings, surgical instruments, disinfectants and cosmetics [6, 7]. However, this increase in the use of AgNPs has raised serious concerns about their potential adverse effects and toxicity on human health [6, 7].

There are several mechanisms through which AgNPs can enter the human body and interact with blood components, either directly, or indirectly. The respiratory system provides a major portal for AgNPs used extensively in healthcare and hygiene sprays [8]. In this context, several animal and human studies have demonstrated significant alveolar-capillary translocation of inhaled nanoparticles via endocytocis or transcytosis [8-10]. In addition, transdermal penetration of nanoparticles has been previously reported [11]. In fact, close contact with AgNPs used as coatings in surgical dressings may allow AgNPs to penetrate the skin barrier and enter the capillaries [8]. AgNPs are also used widely as food preservatives and water disinfectants [12]. Hence, the gastrointestinal system provides another route for AgNPs entry to human body [8]. Other potential route of AgNPs in case of biomedical applications includes parenteral administration, where AgNPs are able to directly interact with blood components [13], including erythrocytes and may potentially induce pathophysiological effects.

Previous studies using diesel exhaust particle (DEP), silica nanoparticles (SiNPs) and lead nanoparticles have demonstrated significant hemolysis and oxidative stress on human, rat and mouse erythrocytes [14-16]. In addition, studies using human erythrocytes have investigated the effects of AgNPs on hemolysis, morphology and their uptake [17, 18]. Nevertheless, the mechanism underlying the pathophysiological effects of AgNPs on erythrocytes physiology is not fully understood.

Several physiochemical properties determine the toxicity of AgNPs including their size, shape and surface chemistry [19]. In addition, coating has been reported to play an important role in NPs toxicity. In this context, *in vivo* studies have reported that polyvinylpyrrolidone (PVP) and citrate (CT) coated AgNPs induce tissue specific toxicity and aggravate cardiac ischemic reperfusion injury [20, 21]. Moreover, a previous *in vitro* study has shown that PVP- and CT- AgNPs induce toxicity in J774A.1 macrophage and HT29 epithelial cells [22]. Also, Huang et al. [23] have investigated the hemolytic effect of PVP- and CT- AgNPs on human erythrocytes. However, to our knowledge, no study has comprehensively evaluated the effect of PVP- and CT- AgNPs on hemolysis, oxidative stress, calcium homeostasis and eryptosis. Hence, the aim of our study was to investigate the mechanism underlying the effect of PVP- and CT- AgNPs, at various concentrations (2.5, 10 and 40 μg/ml), on hemolysis, uptake of AgNPs by erythrocytes, oxidative stress, intracellular calcium, annexin V, caspase 3 and calpain.

Materials and Methods

Particles

Suspensions of silver nanoparticles of 10 nm (BioPure™), coated with either PVP or CT were purchased from NanoComposix (San Diego, CA, USA). The provided stock concentrations were 1.0 mg/ml with endotoxin level <5 EU/ml and silver purity of 99.99%. The zeta potential of PVP- and CT- AgNPs were -26 mV and -33 mV, respectively, and the surface areas were 53.5 m^2/g and 59.0 m^2/g, respectively. The pH of both the suspensions was 7.4. The suspending solvents of PVP- and CT- AgNPs were 0.9% NaCl and 2.0 mM sodium citrate, respectively. To minimize aggregation, the stock particle suspensions were always sonicated for 15 min and vortexed for 30 sec before their dilution, or before incubation with erythrocytes.

Transmission electron microscopy (TEM) of AgNPs

We analyzed the nanoparticle suspension used in our study by TEM. The suspensions were primarily subjected to sonication at room temperature for 15 min prior to processing for TEM. A drop of PVP- and CT-AgNPs suspensions were deposited on a 200 mesh Formvar/Carbon coated copper grid and allowed to dry for 1 h at room temperature. Then the grids were examined and photographed at different magnifications using FEI Tecnai Biotwin Spirit G2 TEM (FEI, Eindhovon, Netherlands).

Animal handling and blood collection

Balb/C mice were housed in light (12 h light:12 h dark cycle) and temperature controlled (22±1 °C) rooms. They had free access to water and standard pellet diet *ad libitum*. All experimental procedures were in accordance with protocols of the Institutional Animal Care and Research Advisory Committee and the project approved by Institutional Review Board of United Arab Emirates University.

Animals were anesthetized intraperitonially with sodium pentobarbital 30 mg/kg, and then blood was drawn from the inferior vena-cava with syringe prewetted with 4% sodium citrate and collected in EDTA (4%) containing tubes. The blood sample was then processed according to the type of experiment conducted.

Preparation of erythrocytes

The method for preparation of erythrocytes used in the present study has been previously described [14, 24]. Briefly, collected mouse blood was mixed by gentle inversion of tube and centrifuged at 1200 *g* for 15 min. The plasma supernatant was discarded, and the erythrocytes were washed 4 times by suspending them in 0.9% NaCl followed by centrifugation at 1200 *g* for 10 mins. The final suspension consisted of 5 % by volume of erythrocyte in saline. Flat bottom well plates were used to incubate 840 µl of erythrocyte with 160 µl of PVP- and CT- coated AgNP suspensions (2.5, 10 and 40 µg/ml). Negative control consisted of 0.9% NaCl and 2 mM Citrate respectively. Positive control consisted of 0.1% Triton X 100. The plates were incubated for 4 h at room temperature under shaded light, shaking gently on an orbital plate shaker. After incubation the samples were transferred to 1.5 ml eppendorf tube and were centrifuged at 1200 *g* for 5 min. The resulting supernatant was collected for hemolysis assay, annexin V and oxidative markers assays. The deposited erythrocytes were fixed with Karnovsky's fixative (2% paraformaldehyde and 2.5% glutaraldehyde in 0.1 M phosphate buffer at 7.2 pH) for TEM.

Hemolysis assay

The hemolysis assay was performed according to previously reported technique [15, 25]. Briefly, erythrocytes incubated with PVP- and CT- AgNPs was centrifuged as described above. After that, 90 µl of the supernatant was added in a 96 well plate and the amount of hemoglobin released was determined spectrophotometrically at a wavelength of 540 nm. The percent hemolysis was calculated using the linear equation $y=mx+c$ where %hemolysis (x) = [(sample optical density (y) – negative control optical density (c))/ (positive control optical density – negative control optical density) (m)] * 100 [14, 24].

Erythrocyte analysis by TEM

Fixed cells were processed according to method described previously [15]. Briefly, the cells were washed with 0.1 M phosphate buffer and for 1 h at room temperature on rotamixer and post fixed with 1% osmium tetraoxide in 100 mM cacodylate buffer. After that cells were dehydrated in a series of graded ethanol concentration, infiltrated with Agar 100 epoxy resin, embedded into resin filled molds and polymerized at 65°C for 24 h. Blocks were trimmed and ultrathin sections were obtained by an ultra-microtome (Leica, Mikrosysteme GmbH, Wien, Austria). Ultrathin sections were collected on 200 mesh Cu grids and were contrasted with uranyl acetate and followed by lead citrate double stain. The grids were examined and photographed at variable magnification by TEM [15, 26].

Measurements of oxidative stress markers

Supernatants were collected after incubation of erythrocytes with PVP- and CT- AgNP (2.5, 10 and 40 µg/ml) by the process described above and was subjected to oxidative stress marker assay. The erythrocytes treated with 0.9% NaCl and 2 mM citrate were taken as control. Erythrocyte malondialdehyde (MDA) was quantified colorimetrically following its controlled reaction with thiobarbituric acid [27] with a commercially available kit (Cayman chemicals, Ann Abror, MI, USA). Reduced glutathione (GSH) concentration (Sigma Chemicals, St Loius, MO, USA) and catalase (CAT) activity (Activity kit, Cayman chemicals, Ann Abror, MI, USA) were analyzed spectrophotometrically according to methods described by the manufacturers.

Measurement of intracellular calcium

Intracellular Ca^{2+} was measured in incubated medium of erythrocytes treated with either vehicle or various concentrations of PVP- and CT- AgNPs according to a previously described technique [28]. Briefly, erythrocytes were washed with saline (0.9% NaCl) four times followed by centrifugation for 10 min at 1200 *g*. The erythrocytes were then resuspended in 1 mM Ringers solution. The final suspension consisted of 0.5% hematocrit of erythrocyte in 1 mM Ringers solution. The cells were then incubated in a flat bottom plate with the AgNPs at 37 °C for 4 h. After that the incubated cell suspensions were collected in eppendorf tube and centrifuged for 5 min at 1200 *g*. The supernatant was discarded, and the cells resuspended in 5mM Ringers solution to which 5 µl of Fura 2AM (Calbiochem; La Jolla, CA, USA) was added and incubated for 15 min at 37 °C in dark on a shaker. After that, the cell suspensions were centrifuged at 1200 *g* for 5 min. The Fura 2AM loaded erythrocytes were resuspended in 1 mM Ringers solution and incubated for 30 min at 37 °C in dark on a shaker. Finally Ca^{2+} - dependent fluorescence intensity was then monitored with a fluorometer (model SFM 25, Kontron; Zurich, Switzerland) set at 340 nm excitation and 510 nm emission [29].

Assessment of Annexin V

Annexin V bound to exposed phosphatidylserine was measured in incubated medium of erythrocytes using mouse ANXA5 ELISA kit according to manufacturer's instruction (Elabscience, Texas, USA).

Caspase 3 analysis

The activity of caspase 3 was determined in incubated medium of erythrocytes using a caspase 3 activity fluorometric assay kit according to manufacturer's instruction (BD Biosciencences, San Jose, CA)

Moreover, caspase 3 expression was analysed by Western blot analysis according to previously described technique [30]. Freshly isolated erythrocytes that were incubated with either vehicle or various concentrations of PVP- or CT- AgNPs, were washed twice in PBS and lysed in 250 µl of radioimmunoprecipitation assay (RIPA) buffer (25 mM Tris-HCl pH 7.6, 150 mM NaCl, 1% NP-40, 1% sodium deoxycholate, 0.1% SDS) containing protease and phosphatase inhibitor. Insolubilized material was removed by centrifugation at 14000 *g* for 15 min. The supernatants were immediately removed and used for protein estimation using a Pierce bicinchoninic acid protein assay kit (Thermo Scientific, Waltham, MA, USA). A 100 µg of protein/ lane was electrophoretically resolved by 12% sodium dodecyl sulfate polyacrylamide gel electrophoresis (SDS-PAGE) and then transferred onto polyvinylidene difluoride membranes. The immunoblots were blocked for 2 h, with 5% nonfat dry milk in 1X Tris-buffered saline containing Tween 20 (1%, v/v) (TBST) and subsequently incubated overnight at 4 °C with rabbit polyclonal caspase-3 antibody (1:1000 dilution, Cell Signalling Technology, Danvers, MA, USA) in 5% w/v nonfat dry milk. The blots were then incubated with goat anti-rabbit IgG horseradish peroxidase (HRP) conjugated secondary antibody (1:5000 dilution, Abcam), for 2 h, at room temperature, and developed using Pierce enhanced chemiluminescent plus Western blotting substrate Kit (Thermo Scientific). The densitometric analysis of the protein bands was performed for caspase-3 with Typhoon FLA 9500 (GE Healthcare Bio-Sciences AB, Uppsala, Sweden). Blots were then re-probed with mouse monoclonal β-actin HRP conjugated antibody (1:1000 dilution, Santa Cruz Biotechnology, Dallas, Texas, U.S.A) and used as a loading control.

Measurement of calpain activity

The activated calpain in cytosol of incubated erythrocytes was flurometrically determined using a calpain activity assay kit according to manufacturer's instruction (Genway Biotech, San Diego, USA).

Statistics

All statistical analyses were performed with GraphPad Prism Software version 7 (San Diego, CA, USA) and the data and figures were reported as mean ± SEM. Comparisons between groups were performed by one-way analysis variance (ANOVA) followed by Dunnett's multiple range test. P-values <0.05 were considered as significant.

Results

Characterization of PVP- and CT- AgNPs

The morphology and particle size of PVP- and CT- AgNPs were determined by TEM are shown in Fig. 1. TEM analysis of PVP- and CT- AgNPs revealed homogenous particle size of approximately 10 nm in diameter and this corroborates the size provided by the manufacturer. Both types of AgNPs were spherical in shape.

Effect of AgNPs on erythrocyte hemolysis

Fig. 2 shows the hemolytic effect of AgNPs on erythrocytes. Incubation of erythrocytes with AgNPs caused a dose-dependent hemolysis. The effects were significant at concentrations of 10 µg/ml ($P<0.001$) and 40 µg/ml ($P<0.001$) for PVP- AgNPs and at a concentration of 40 µg/ml ($P<0.001$) for CT- AgNPs compared with their respective controls. The degree of hemolysis observed at concentration of 2.5, 10 and 40 µg/ml for PVP- AgNPs were 0.99%, 3.96% and 16.34% and those observed for CT- AgNPs were 2.43%, 2.67% and 16.67% respectively.

Erythrocyte analysis by EM

TEM images of erythrocytes incubated with PVP- and CT- AgNPs at concentration of 2.5, 10 and 40 µg/ml are shown in Fig. 3. Both types of AgNPs were found to be taken up by erythrocytes at all tested concentrations. In the erythrocytes the AgNPs were located both within as well as on the margins.

Effect of AgNPs on concentrations of MDA and GSH and CAT activity

Concentrations of MDA, GSH and measurement of CAT activity are shown in Fig. 4. MDA was used to assess the susceptibility of erythrocytes lipid peroxidation *in vitro*. Compared with their respective controls, the MDA concentration was dose-dependently increased by the incubation of erythrocytes with various concentrations of PVP- and CT- AgNPs (Fig. 4A). However, the level of significance was only achieved at highest tested concentration, i.e. 40 µg/ml ($P<0.001$) for both PVP-and CT- AgNPs. Fig. 4B shows the effect of AgNPs on concentration of GSH. Compared with control, the concentration of GSH was significantly decreased. The level of significance was achieved at all studied concentrations ($P<0.001$) for both PVP- and CT- AgNPs. Likewise, compared with their respective controls, there was a significant decrease of catalase activity in erythrocytes incubated with PVP and CT- AgNPs at all tested concentrations ($P<0.001$) as shown in Fig. 4C.

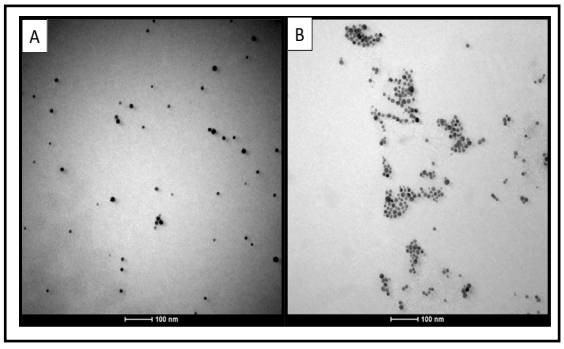

Fig. 1. Transmission electron microscope (TEM) analysis of polyvinylpyrrolidone (A) or citrate (B) coated silver nanoparticles.

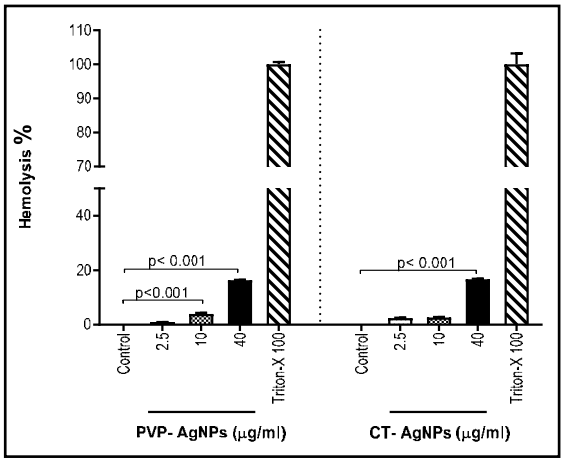

Fig. 2. Hemolytic effect of polyvinylpyrrolidone (PVP) and citrate (CT) silver nanoparticles (AgNPs) in incubated mouse erythrocytes. The results are expressed as % of postive control (0.1% Triton-X 100). Data are mean± SEM (n=8 in each group). Statistical analysis by one-way ANOVA followed by Dunnett's multiple range test.

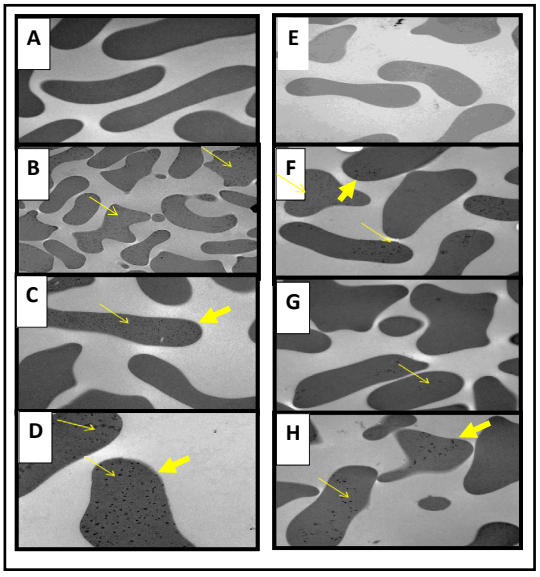

Fig. 3. Transmission electron microscope (TEM) analysis of erythrocytes after in vitro incubation with saline (control, A), polyvinylpyrrolidone (PVP) silver nanoparticles (AgNPs) 2.5, 10, 40 µg/ml (B, C, D respectively), 2 mM citrate (control, E) or citrate (CT) coated AgNPs 2.5, 10, 40 µg/ml (F, G, H respectively). AgNPs are localized within (thin arrows) as well as on the margins (thick arrows) of the erythrocytes

Effect of AgNPs on intracellular calcium

Fig. 5 illustrates the effect of various concentrations of PVP- and CT- AgNPs on cytosolic calcium concentration from Fluro3 fluorescence. The incubation of erythrocytes with AgNPs caused a dose-dependent increase in cytosolic calcium concentration compared with control. While the level of significance was achieved at 10 and 40 µg/ml (P<0.001) for PVP- AgNPs, the CT-AgNPs showed increased cytosolic calcium concentration at all tested dose, i.e. 2.5, 10, and 40 µg/ml (P<0.001).

Effect of AgNPs on annexin V-binding

Exposure of phosphatidylserine at the cell surface was estimated from bound annexin V. Incubation of erythrocyte with PVP- and CT- AgNPs triggered annexin V binding as shown in Fig. 6. The effect was significant at concentration of 2.5 µg/ml (P<0.05), 10 µg/ml (P<0.001) and 40 µg/ml (P<0.001) of PVP- AgNPs. The effect of CT- AgNPs was also significant at all concentrations used, i.e. 2.5, 10 and 40 µg/ml (P<0.001).

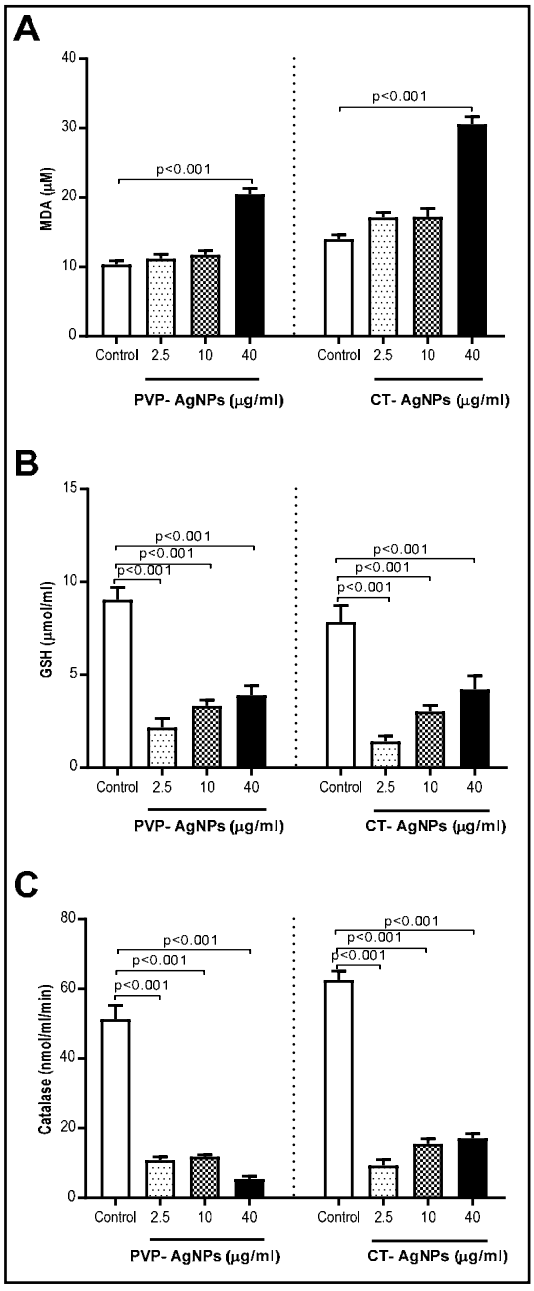

Fig. 4. Effect of polyvinylpyrrolidone (PVP) and citrate (CT) silver nanoparticles (AgNPs) on concentration of malonaldialdehyde (MDA, A), reduced glutathione (GSH, B) and catalase activity (C) measured in the incubation medium of erythrocytes. Data are mean± SEM (n=8 in each group). Statistical analysis by one-way anova followed by Dunnett's multiple range test.

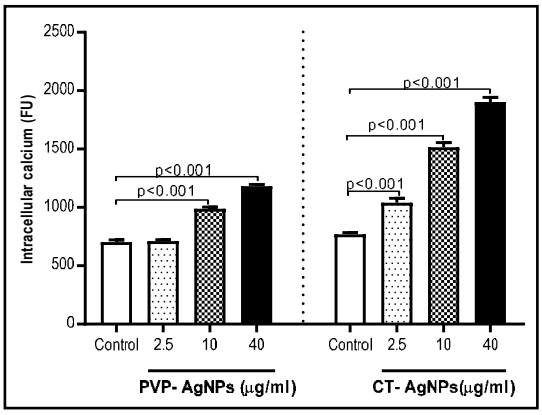

Fig. 5. Effect of polyvinylpyrrolidone (PVP) and citrate (CT) silver nanoparticles (AgNPs) on intracellular calcium concentration measured in incubated erythrocytes. Data are mean± SEM (n=8 in each group). Statistical analysis by one-way anova followed by Dunnett's multiple range test.

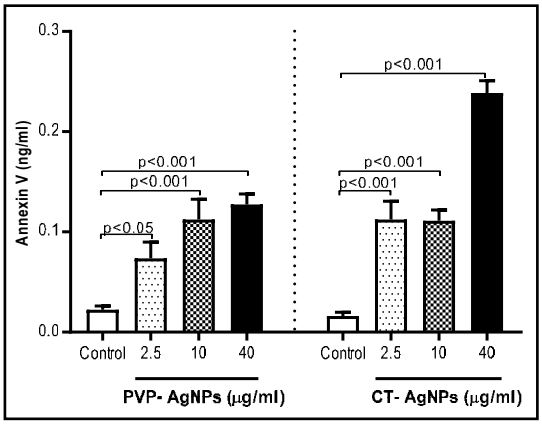

Fig. 6. Effect of polyvinylpyrrolidone (PVP) and citrate (CT) silver nanoparticles (AgNPs) on the concentration of bound Annexin V in the incubation medium of erythrocytes. Data are mean± SEM (n=8 in each group). Statistical analysis by one-way anova followed by Dunnett's multiple range test.

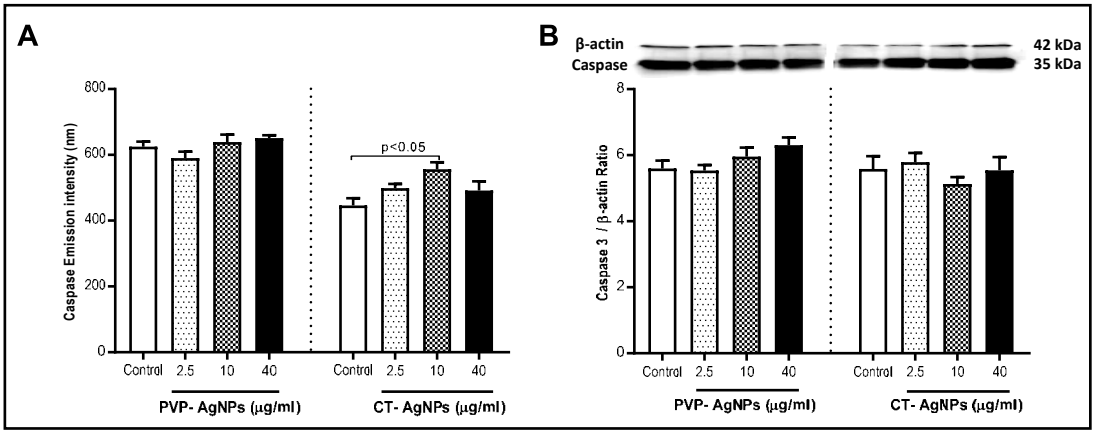

Fig. 7. Effect of polyvinylpyrrolidone (PVP) and citrate (CT) silver nanoparticles (AgNPs) on erythrocyte caspase 3 activity (A) and caspase 3 expression assessed by western blotting (B). Data are mean± SEM (n=7-8 in each group). Statistical analysis by one-way anova followed by Dunnett's multiple range test.

Effect of AgNPs on caspase 3 activity and expression

The assessments of caspase 3 activity and expression in erythrocytes following exposure to various concentrations of PVP- or CT- AgNPs is represented in Fig. 7. Overall, there was no effect of both PVP- and CT- AgNPs on casapse activity in incubated erythrocytes. Compared with the control group, only CT- AgNPs showed a significant increase at a dose 10 μg/ml ($P<0.05$). Likewise, compared with the control group, the western blot analysis showed no statistically significant effect of various concentrations of PVP- or CT- AgNPs on total caspase 3 expression in erythrocytes.

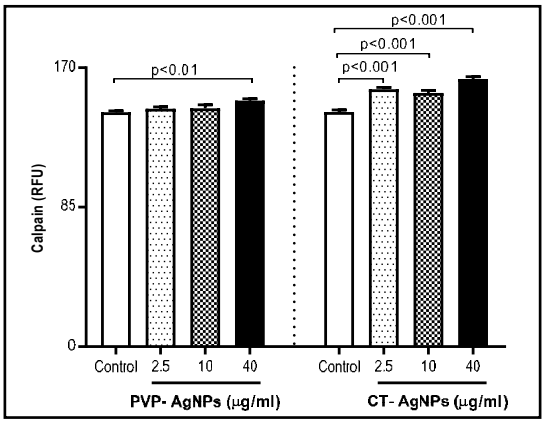

Fig. 8. Effect of polyvinylpyrrolidone (PVP) and citrate (CT) silver nanoparticles (AgNPs) on calpain activity measured in incubated erythrocytes. Data are mean± SEM (n=8 in each group). Statistical analysis by one-way anova followed by Dunnett's multiple range test.

Effect of AgNPs on calpain activity

Detection of activated calpain in cytosol upon incubation of erythrocytes with PVP- and CT- AgNPs is shown in Fig. 8. Compared with the control, the incubation of erythrocytes with PVP- AgNPs caused a significant increase in calpain activity at dose 40 μg/ml ($P<0.01$), and incubation with CT- AgNPs caused a significant increase in calpain activity at all concentrations used, i.e. 2.5, 10 and 40 μg/ml ($P<0.001$).

Discussion

In this work, we assessed the *in vitro* effects of PVP- and CT- AgNPs on mouse erythrocytes and showed that AgNPs can induce hemolysis, oxidative stress and increase cytosolic Ca^{2+}, annexin V binding and calpain activity.

Our *in vitro* erythrocyte study is relevant to previous *in vivo* studies which demonstrated that exposure to AgNPs is associated with cardiovascular dysfunction in addition to cytotoxicity and oxidative stress [20, 21]. We incubated the erythrocytes with vehicle or PVP- or CT- AgNPs for 4 h; a time point similar to previous *in vitro* studies [18, 31]. The various concentrations of PVP- and CT- AgNPs (2.5, 10 and 40 μg/ml) used in our study are also similar to previous studies evaluating nanotoxicity and blood compatibility of erythrocytes incubated with AgNPs [17, 23]. Our concentrations are comparable with previous studies using AgNPs on human, mouse and fish erythrocytes and the highest dose of 40 μg/ml, is much lower than the optimal dose of AgNPs (200 μg/ml) that has been reported to induce hemolysis in human erythrocytes [17, 18, 23, 32-34]. In fact, in humans following oral exposure, *in vivo* serum concentration of AgNPs of up to 10μg/ml has been reported [35, 36]. The latter is within the range of concentrations of AgNPs that we used in our present study. Both particle size and coating have been reported to play critical role in NP-induced toxicity; size <50 nm AgNPs induces greater hemolysis and increased uptake by erythrocytes [17, 22, 23, 34]. Hence, we presently assessed the impact of 10 nm AgNPs with 2 different coating, namely PVP and CT.

Our hemolytic assay results show that both 10 nm PVP- and CT- AgNPs cause a dose-dependent hemolysis. Similar results were obtained when fish and human erythrocytes were incubated with various sizes of AgNPs (15 nm – 100 nm); the highest hemolytic activity being observed with size <50 nm AgNPs [17, 18]. Huang et al. [23], in a study using human erythrocytes demonstrated that PVP- AgNPs (20 nm) caused ~19% hemolysis while CT- AgNPs (20 nm) caused ~10% hemolysis at the concentration of 40 μg/ml. Research focusing on TiO_2 also showed evidence of hemolysis in rabbit erythrocytes [37]. Our previous studies on interaction of erythrocytes with DEP and amorphous SiNPs demonstrated significant dose-dependent hemolysis [14, 15]. Besides using Triton X 100 as a positive control, we have also assessed the hemolytic effects of a positive control particle, namely amorphous SiNPs (50 nm), at a dose of 25 μg/ml [15]. The latter results confirmed the hemolytic effect of SiNPs (data not shown). The hemolytic activity of SiNPs exposed erythrocytes has been demonstrated to be dependent on presence of negatively charged silanol groups [38]. However, the mechanism by which AgNPs may induce hemolysis is not fully understood.

There is a strong body of evidence suggesting interaction of RBC with AgNPs itself can induce hemolysis, rather than released silver ion mediated cellular toxicity [17, 18]. It has been also stated that AgNPs can bind to thiol groups within proteins or phospholipids of membrane with high affinity and thereby promote denaturation [39]. Moreover, interaction of negatively charged silver surface with cations in membrane of RBC may also contribute to hemolysis [39].

To obtain more information about the possible uptake and localization of AgNPs within RBCs, TEM analysis has been performed following incubation of erythrocytes with various concentrations of AgNPs. Interestingly, both 10 nm PVP- and CT- AgNPs were observed within the erythrocytes even at our lowest concentration of AgNPs that is 2.5 μg/ml. The optimal size for uptake of AgNPs by fish erythrocytes was reported to be ~50 nm [17]. However, despite the presence of AgNPs in the erythrocytes the degree of hemolysis observed was relatively slight for the concentrations of 2.5 μg/ml and 10 μg/ml for CT-AgNPs and concentration of 2.5 μg/ml for PVP- AgNPs. This could probably suggest that the hemolytic effect is both coating and dose dependent. Our previous studies showed that DEP and SiNPs are taken up by erythrocytes [14, 15]. Geiser et al. [40], in studies of TiO2 NPs on lung cells and erythrocytes showed that particle uptake in cells was by diffusion or adhesive interactions rather than endocytosis. However, it is well established that RBC's lack endocytic machinery and there is no actin myosin system [41], and therefore the mechanism underlying the uptake of nanoparticle by erythrocytes may be different from other phagocytic cells. Though our study does not clearly define the mechanism of entry of AgNPs into the cell it could be possible that, given their very small size, the 10 nm AgNPs were able to enter the erythrocytes via diffusion as suggested before [19]. Further studies are required to clarify this particular point.

To further clarify the possible mechanism related to hemolytic effect of PVP- and CT-AgNPs, we assessed biomarkers of oxidative stress including MDA, GSH concentration and CAT activity. MDA is one of the final products of polyunsaturated fatty acid peroxidation in the cells and is used as a marker of cell membrane injury as its production is increased with increase in free radicals [27]. Our data showed a dose-dependent increase of MDA with significance at the highest concentration 40 μg/ml for both PVP- and CT- AgNPs. Previous *in vitro* hemolytic studies also demonstrated significant and dose-dependent increase in MDA in fish erythrocyte incubated with AgNPs (15 nm - 100 nm) at various concentrations (1.25 μg/ml – 20 μg/ml) [17]. However, our previous study of interaction of DEP with erythrocytes demonstrated no significant changes of MDA in mouse erythrocytes at 100 μg/ml [14]. In contrast, our other study on interaction of erythrocytes with SiNPs showed significant MDA increase even at 25 μg/ml [15]. These results collectively indicate that the overproduction of MDA in erythrocytes is particle and dose-dependent and that both studied coating (PVP and CT) induce lipid peroxidation of RBC. Oxidative stress results from imbalance between reactive oxygen species (ROS) and the antioxidant defense system. Erythrocyte antioxidant enzymes are major circulating antioxidant enzymes in the oxidative stress defense system [42]. GSH and CAT are major enzymes that control the biological effect of ROS [42]. While GSH quenches the free radicals by serving as electron donor, CAT converts hydrogen peroxide to water and oxygen [43]. Our data show, incubation with AgNPs results in significant decrease in GSH concentration and CAT activity compared to control. The decrease of antioxidants in the present study can be attributed to the increase of their consumption due to increase in ROS. The activity of CAT has been shown to be decreased, and the concentrations of GSH and MDA increased in trout hepatocytes incubated with selenomethionine [44]. The data of our previous study showed a significant and dose - dependent increase in CAT activity and GSH concentrations in erythrocytes treated with SiNPs [15]. The latter effect has been explained by an adaptive response that counterbalances the potentially damaging activity of free oxygen radicals by antioxidant defense mechanism [15]. Overall, these results indicate the relation between AgNPs interaction and alteration in oxidative stress and antioxidant enzymes activities.

Mature erythrocytes are highly specialized cells that lack normal cell organelles, such as nucleus and mitochondria, which are vital for the regulation of apoptosis, an innate mechanism of cell clearance [45]. The senescence involved in mature erythrocytes, is characterized by distinct changes in shape and plasma membrane with translocation of phosphatidylserine from the inner leaflet of cell membrane, and is termed as eryptosis [46, 47]. The later has been evaluated using various techniques including cytoflurometric

analysis [48]. However, unlike apoptosis of erythroblast that is caspase - dependent, the mature erythrocyte is driven into eryptosis by increase in intracellular calcium which in turn triggers activation of calpain [47]. Apoptosis mediated cell death via AgNPs exposure has previously been demonstrated in various cell line including normal human lung fibroblast, gliobastoma and osteoblastic cells [49]. However, little is known about the mechanism of cell death in AgNPs - treated erythrocytes. Our data shows significant and dose dependent increase of intracellular calcium and Annexin V binding for both PVP- and CT- AgNPs. It has been shown that increased calcium activity is due to activation of Ca^{2+} permeable cation channels which is, in turn, triggered by erythrocyte injury including oxidative stress [46]. Additionally, typical features of eryptosis including cell shrinkage, membrane blebbing, phoshphotidylserine externalization has been reported in erythrocytes exposed to Ca^{2+} ionophore ionomycin or A23187 [50, 51]. Annexin V is a Ca^{2+}-dependent cellular protein that has the ability to bind with phosphotidylserine and used as an apoptotic marker when exposed on outer leaflet of cell membrane [50, 52]. Our present findings also corroborates our previous study that demonstrated increased erythrocyte cytosolic calcium and annexin V binding following incubation with SiNPs [15]. However, unlike the previous study, there were no significant changes in caspase 3 activity compared to control except for CT- AgNPs at concentration of 10 µg/ml. The discrepancy between the present and the previous study could be related to type of NPs (PVP- and CT- AgNPs versus SiNPs) and/or size of NPs (10 nm versus 50 nm). The caspase activity results were further confirmed by western blot analysis, which also showed no significant changes in expression of the total caspase 3 in erythrocytes exposed to various concentration of PVP- or CT- AgNPs, compared with controls. Caspase members contain a cystine residue and exists as zymogens that needs to undergo proteolytic cleavage before inducing its initiator or effector function in apoptosis [53]. Though the presence of caspase is well established in erythrocyte, their role in eryptosis is not clearly defined [45]. Berg et al. [54] suggested that the inability of caspase activation in erythrocyte might be due to presence of novel inhibitor or lack of other elements of apoptotic machinery like Apaf1 and cytochrome C. Similar to caspases, another calcium dependent cystine protease, calpains, exits as proenzymes and is reported to play a role in eryptosis [55]. Our data show that the incubation of erythrocytes with PVP- or CT-AgNPs, results in significant increase in calpain activity compared with control, and this increase could be attributed to the increase in cytosolic calcium. Our findings corroborates with a previous study which demonstrated that changes in intracellular calcium led to the activation of calpain [54].

To conclude, the interaction of two differently coated AgNPs was comprehensively investigated in an *in vitro* model of mouse erythrocytes. We observed that both PVP- and CT-AgNPs caused hemolysis and were taken up by the erythrocytes at all tested concentrations. We also demonstrated that PVP- and CT- AgNPs induced oxidative stress and increased cytosolic calcium, annexin V binding and calpain activity which may explain the cause of hemolysis and mechanism by which eryptosis may be triggered. More studies are required to further investigate the mechanism underlying pathophysiological effects of AgNPs on eryptosis.

Acknowledgements

This work was supported by funds of the College of Medicine and Health Sciences, United Arab Emirates University (UAEU) grant and UAEU-SQU grant.

Disclosure Statement

The authors declare to have no competing interests.

References

1 Hett A: Nanotechnology-primarily an order of magnitude; in Hett A: Nanotechnology: Small matter, many unknowns. Swiss Reinsurance Company, 2004, pp 11-13.

2 Nemmar A, Holme JA, Rosas I, Schwarze PE, Alfaro-Moreno E: Recent advances in particulate matter and nanoparticle toxicology: a review of the *in vivo* and *in vitro* studies. Biomed Res Int 2013;2013:2314-6133.
3 Bhatia S: Nanoparticles Types, Classification, Characterization, Fabrication Methods and Drug Delivery Applications; in Bhatia S: Natural Polymer Drug Delivery Systems. Springer, Cham, 2016, pp 33-93.
4 Felice B, Prabhakaran MP, Rodriguez AP, Ramakrishna S: Drug delivery vehicles on a nano-engineering perspective. Mater Sci Eng C Mater Biol Appl 2014;41:178-195.
5 Sharma VK, Yngard RA, Lin Y: Silver nanoparticles: green synthesis and their antimicrobial activities. Adv Colloid Interface Sci 2009;145:83-96.
6 Natsuki J, Natsuki T, Hashimoto Y: A review of silver nanoparticles: synthesis methods, properties and applications. Inter J Mat Sci Appl 2015;4:325-332.
7 Tran QH, Quy Nguyen V, Le AT: Silver nanoparticles: synthesis, properties, toxicology, applications and perspectives. Adv Nat Sci Nanosci Nanotechnol 2013;4:033001.
8 Chen X, Schluesener HJ: Nanosilver: a nanoproduct in medical application. Toxicol Lett 2008;176:1-12.
9 Shimada A, Kawamura N, Okajima M, Kaewamatawong T, Inoue H, Morita T: Translocation pathway of the intratracheally instilled ultrafine particles from the lung into the blood circulation in the mouse. Toxicol Pathol 2006;34:949-957.
10 Kato T, Yashiro T, Murata Y, Herbert DC, Oshikawa K, Bando M, Ohno S, Sugiyama Y: Evidence that exogenous substances can be phagocytized by alveolar epithelial cells and transported into blood capillaries. Cell Tissue Res 2003;311:47-51.
11 Lademann J, Weigmann H-J, Rickmeyer C, Barthelmes H, Schaefer H, Mueller G, Sterry W: Penetration of titanium dioxide microparticles in a sunscreen formulation into the horny layer and the follicular orifice. Skin Pharmacol Appl Skin Physiol 1999;12:247-256.
12 Zhang YY, Sun J: A study on the bio-safety for nano-silver as anti-bacterial materials. Zhongguo Yi Liao Qi Xie Za Zhi 2007;31:36-38.
13 Yah CS, Simate GS, Iyuke SE: Nanoparticles toxicity and their routes of exposures. Pak J Pharm Sci 2012;25:477-491.
14 Nemmar A, Zia S, Subramaniyan D, Al-Amri I, Al Kindi MA, Ali BH: Interaction of diesel exhaust particles with human, rat and mouse erythrocytes *in vitro*. Cell Physiol Biochem 2012;29:163-170.
15 Nemmar A, Beegam S, Yuvaraju P, Yasin J, Shahin A, Ali BH: Interaction of amorphous silica nanoparticles with erythrocytes *in vitro*: role of oxidative stress. Cell Physiol Biochem 2014;34:255-265.
16 Kim CB, Shin S, Song SH: Hemorheological changes caused by lead exposure. Clin Hemorheol Microcirc 2013;55:341-348.
17 Chen LQ, Fang L, Ling J, Ding CZ, Kang B, Huang CZ: Nanotoxicity of silver nanoparticles to red blood cells: size dependent adsorption, uptake, and hemolytic activity. Chem Res Toxicol 2015;28:501-509.
18 Kim MJ, Shin S: Toxic effects of silver nanoparticles and nanowires on erythrocyte rheology. Food Chem Toxicol 2014;67:80-86.
19 Shang L, Nienhaus K, Nienhaus GU: Engineered nanoparticles interacting with cells: size matters. J Nanobiotechnology 2014;12:5.
20 Recordati C, De Maglie M, Bianchessi S, Argentiere S, Cella C, Mattiello S, Cubadda F, Aureli F, D'Amato M, Raggi A: Tissue distribution and acute toxicity of silver after single intravenous administration in mice: nano-specific and size-dependent effects. Part Fibre Toxicol 2016;13:12.
21 Holland NA, Thompson LC, Vidanapathirana AK, Urankar RN, Lust RM, Fennell TR, Wingard CJ: Impact of pulmonary exposure to gold core silver nanoparticles of different size and capping agents on cardiovascular injury. Part Fibre Toxicol 2016;13:48.
22 Nguyen KC, Seligy VL, Massarsky A, Moon TW, Rippstein P, Tan J, Tayabali AF: Comparison of toxicity of uncoated and coated silver nanoparticles. J Phys Conf Ser 2013;429:012025.
23 Huang H, Lai W, Cui M, Liang L, Lin Y, Fang Q, Liu Y, Xie L: An evaluation of blood compatibility of silver nanoparticles. Sci Rep 2016;6:25518.
24 Lu S, Duffin R, Poland C, Daly P, Murphy F, Drost E, MacNee W, Stone V, Donaldson K: Efficacy of simple short-term *in vitro* assays for predicting the potential of metal oxide nanoparticles to cause pulmonary inflammation. Environ Health Perspect 2009;117:241.
25 Neun BW, Dobrovolskaia MA: Method for analysis of nanoparticle hemolytic properties *in vitro*. Nano Lett 2011:215-224.
26 Nemmar A, Al-Maskari S, Ali BH, Al-Amri IS: Cardiovascular and lung inflammatory effects induced by systemically administered diesel exhaust particles in rats. Am J Physiol 2007;292:L664-L670.
27 Lefevre G, Beljean-Leymarie M, Beyerle F, Bonnefont-Rousselot D, Cristol JP, Therond P, Torreilles J: Evaluation of lipid peroxidation by measuring thiobarbituric acid reactive substances. Ann Biol Clin 1998;56:305-319.

28 Foller M, Mahmud H, Gu S, Wang K, Floride E, Kucherenko Y, Luik S, Laufer S, Lang F: Participation of leukotriene C4 in the regulation of suicidal erythrocyte death. Acta Physiol Pol 2009;12:135.
29 Pignatelli P, Lenti L, Sanguigni V, Frati G, Simeoni I, Gazzaniga PP, Pulcinelli FM, Violi F: Carnitine inhibits arachidonic acid turnover, platelet function, and oxidative stress. Am J Physiol 2003;284:H41-H48.
30 Walsh M, Lutz RJ, Cotter TG, O'Connor R: Erythrocyte survival is promoted by plasma and suppressed by a Bak-derived BH3 peptide that interacts with membrane-associated Bcl-XL. Blood 2002;99:3439-3448.
31 Choi J, Reipa V, Hitchins VM, Goering PL, Malinauskas RA: Physicochemical Characterization and *In Vitro* Hemolysis Evaluation of Silver Nanoparticles. Toxicol Sci 2011;123:133-143.
32 Krajewski S, Prucek R, Panacek A, Avci-Adali M, Nolte A, Straub A, Zboril R, Wendel HP, Kvitek L: Hemocompatibility evaluation of different silver nanoparticle concentrations employing a modified Chandler-loop *in vitro* assay on human blood. Acta Biomater 2013;9:7460-7468.
33 Shrivastava R, Kushwaha P, Bhutia YC, Flora SJS: Oxidative stress following exposure to silver and gold nanoparticles in mice. Toxicol Ind Health 2016;32:1391-1404.
34 Kwon T, Woo HJ, Kim YH, Lee HJ, Park KH, Park S, Youn B: Optimizing hemocompatibility of surfactant-coated silver nanoparticles in human erythrocytes. J Nanosci Nanotechnol 2012;12:6168-6175.
35 Munger MA, Radwanski P, Hadlock GC, Stoddard G, Shaaban A, Falconer J, Grainger DW, Deering-Rice CE: *In vivo* human time-exposure study of orally dosed commercial silver nanoparticles. Nanomedicine 2014;10:1-9.
36 Smock KJ, Schmidt RL, Hadlock G, Stoddard G, Grainger DW, Munger MA: Assessment of orally dosed commercial silver nanoparticles on human ex vivo platelet aggregation. Nanotoxicology 2014;8:328-333.
37 Li S-Q, Zhu RR, Zhu H, Xue M, Sun XY, Yao SD, Wang SL: Nanotoxicity of TiO 2 nanoparticles to erythrocyte *in vitro*. Food Chem Toxicol 2008;46:3626-3631.
38 Zhao Y, Sun X, Zhang G, Trewyn BG, Slowing II, Lin VSY: Interaction of mesoporous silica nanoparticles with human red blood cell membranes: size and surface effects. ACS Nano 2011;5:1366-1375.
39 Johnston HJ, Hutchison G, Christensen FM, Peters S, Hankin S, Stone V: A review of the *in vivo* and *in vitro* toxicity of silver and gold particulates: particle attributes and biological mechanisms responsible for the observed toxicity. Crit Rev Toxicol 2010;40:328-346.
40 Geiser M, Rothen-Rutishauser B, Kapp N, Schürch S, Kreyling W, Schulz H, Semmler M, Im Hof V, Heyder J, Gehr P: Ultrafine particles cross cellular membranes by nonphagocytic mechanisms in lungs and in cultured cells. Environ Health Perspect 2005;113:1555.
41 Underhill DM, Ozinsky A: Phagocytosis of microbes: complexity in action. Annu Rev Immunol 2002;20:825-852.
42 Bogdanska JJ, Korneti P, Todorova B: Erythrocyte superoxide dismutase, glutathione peroxidase and catalase activities in healthy male subjects in Republic of Macedonia. Bratisl Lek Listy 2003;104:108-114.
43 Shiva Shankar Reddy CS, Subramanyam MVV, Vani R, Devi SA: *In vitro* models of oxidative stress in rat erythrocytes: effect of antioxidant supplements. Toxicol *In vitro* 2007;21:1355-1364.
44 Misra S, Hamilton C, Niyogi S: Induction of oxidative stress by selenomethionine in isolated hepatocytes of rainbow trout (Oncorhynchus mykiss). Toxicol *In vitro* 2012;26:621-629.
45 Holcik M: Do mature red blood cells die by apoptosis? Trends Genet 2002;18:121.
46 Lang F, Lang KS, Lang PA, Huber SM, Wieder T: Mechanisms and significance of eryptosis. Antioxid Redox Signal 2006;8:1183-1192.
47 Daugas E, Cande C, Kroemer G: Erythrocytes: death of a mummy. Cell Death Differ 2001;8:1131-1133.
48 Jemaà M, Fezai M, Bissinger R, Lang F: Methods Employed in Cytofluorometric Assessment of Eryptosis, the Suicidal Erythrocyte Death. Cell Physiol Biochem 2017;43:431-444.
49 Rosário F, Hoet P, Santos C, Oliveira H: Death and cell cycle progression are differently conditioned by the AgNP size in osteoblast-like cells. Toxicology 2016;368:103-115.
50 Föller M, Huber SM, Lang F: Erythrocyte programmed cell death. IUBMB life 2008;60:661-668.
51 Lang F, Birka C, Myssina S, Lang KS, Lang PA, Tanneur V, Duranton C, Wieder T, Huber SM: Erythrocyte ion channels in regulation of apoptosis. Adv Exp Med Biol 2004;559:211-217.
52 Pretorius E, du Plooy JN, Bester J: A comprehensive review on eryptosis. Cell Physiol Biochem 2016;39:1977-2000.
53 Bratosin D, Estaquier J, Petit F, Arnoult D, Quatannens B, Tissier JP, Slomianny C, Sartiaux C, Alonso C, Huart JJ: Programmed cell death in mature erythrocytes: a model for investigating death effector pathways operating in the absence of mitochondria. Cell Death Differ 2001;8:1143.
54 Berg CP, Engels IH, Rothbart A, Lauber K, Renz A, Schlosser SF, Schulze-Osthoff K, Wesselborg S: Human mature red blood cells express caspase-3 and caspase-8, but are devoid of mitochondrial regulators of apoptosis. Cell Death Differ 2001;8:1197-1206.
55 Lang F, Lang E, Föller M: Physiology and pathophysiology of eryptosis. Transfus Med Hemother 2012;39:308-314.